

Statistical comparison of MISR, ETM+ and MODIS land surface reflectance and albedo products of the BARC land validation core site, USA

H. FANG*, S. LIANG, M. CHEN

Department of Geography, University of Maryland, College Park, MD, USA

C. WALTHALL and C. DAUGHTRY

Hydrology and Remote Sensing Laboratory, USDA–ARS, Beltsville, MD, USA

(Received 18 February 2002; in final form 4 February 2003)

Abstract. The Multi-angle Imaging Spectroradiometer (MISR) and Moderate Resolution Imaging Spectroradiometer (MODIS) onboard the National Aeronautics and Space Administration (NASA)'s Earth Observing System (EOS) Terra satellite are crucial for generation of other products such as the Fraction of Photosynthetically Active Radiation (FPAR) and Leaf Area Index (LAI). The analysis reported here compares the reflectance and albedo products from MODIS (MOD09 and MOD43B3), MISR and Landsat Enhanced Thematic Mapper (ETM)+ data using general statistical methods. Four MISR land surface products are examined: hemispherical–directional reflectance factors (HDRF), bidirectional reflectance factors (BRF), bi-hemispherical reflectance (BHR) and directional–hemispherical reflectance (DHR). Ground measurements were used to validate ETM+ reflectance and albedo products (30 m) which were then upscaled and compared with MISR products (1.1 km). The results from 11 May 2000, 5 December 2000 and 22 January 2001 show that: (1) under clear-sky conditions, MISR BRF and HDRF, BHR and DHR are nearly the same ($R^2 > 99\%$); (2) there are strong correlations between ETM+ surface reflectance and MISR nadir-view BRF; however, the relationship is affected by the cloud, snow and shadow; (3) in clear areas, MISR BRF is similar to MOD09, but is greater for the haze and snow regions and smaller for shadows; and (4) the MISR albedo product is closely related to the ETM+ and, to a lesser extent, MODIS.

1. Introduction

The Multi-angle Imaging Spectroradiometer (MISR) is one of the instruments onboard the National Aeronautics and Space Administration (NASA)'s Earth Observing System (EOS) Terra satellite. MISR views the sunlit Earth simultaneously in four spectral bands at nine widely spaced angles ($0, \pm 26.1,$

*Corresponding author; tel: +1-301-405-4050; fax: +1-301-314-9299. e-mail: fanghl@geog.umd.edu

± 45.6 , ± 60.0 and $\pm 70.5^\circ$). The MISR science team produces a series of geophysical products, such as top-of-atmosphere (TOA) albedos, tropospheric aerosol optical depth, TOA and surface bidirectional reflectance factors (BRF), and other related parameters (Diner *et al.* 1999). At the same time, the Moderate Resolution Imaging Spectroradiometer (MODIS) onboard Terra is providing data for surface reflectance, BRF and albedo products because of its large field of view (FOV) (Strahler *et al.* 1999, Vermote and Vermeulen 1999). Surface reflectance and albedo can also be obtained from Landsat Enhanced Thematic Mapper (ETM+) data after removing the atmospheric effects (Liang 2001). These reflectance products are important inputs for the generation of other land products such as vegetation indices (VI), land cover, and the Fraction of Photosynthetically Active Radiation/Leaf Area Index (FPAR/LAI). Users of these products need to know the relative uncertainties associated with the sources of information. The comparison of information products from different satellites has been an important part of validating these products before the information is provided to the user community (Liang *et al.* 2002a).

The goal of this investigation is to compare the land surface albedo and BRF obtained from MISR data with those from MODIS and ETM+ data. This comparison (1) offers an examination of the significance of the differences between these products; (2) offers an assessment and understanding of the reasons for such differences; and (3) provides indications of the impact of the differences to potential users of the product. The hemispherical-directional reflectance factors (HDRF), BRF, bi-hemispherical reflectance (BHR), and directional-hemispherical reflectance (DHR) land surface products are considered by this comparison. DHR is the radiant exitance divided by irradiance under illumination from a single direction. BHR is the radiant exitance divided by irradiance under the same illumination conditions (Diner *et al.* 1999). BHR can be directly determined through field measurements while the DHR needs numerical integration calculation after the BRF is obtained. BRF is defined as the surface-leaving radiance divided by radiance from a Lambertian reflector illuminated from a single direction. HDRF is defined as the surface-leaving radiance divided by radiance from a Lambertian reflector with the same illumination (Diner *et al.* 1999). The differences between BRF and HDRF have been detailed by Gu and Guyot (1993).

Previous work has compared the bidirectional reflectance and albedo of MODIS and MISR (Lucht 1998) using simulated data. Our analysis (figure 1) used satellite data and includes the examination of spatial and temporal product trends, comparison of data products, comparisons with *in situ* data collected over a range of validation sites, and comparisons with data and products were from other spaceborne sensors. First, the characteristics of MISR reflectance and albedo products are examined; secondly, the reflectance differences between BRF and HDRF are numerically evaluated; and thirdly, the albedo difference between BHR and DHR examined. MISR land surface BRF/HDRF products were compared with Landsat7/ETM+ and MODIS surface reflectance products, and land surface broadband albedos converted from MISR BHR/DHR with those from ETM+/MODIS spectral albedos. Although validation depends on ground measurements as the 'truth' for comparisons, there is a significant scale mismatch between ground instruments and MISR resolutions. Since it is difficult to find a large, homogeneous surface at the MISR resolution (1.1 km), we rely on ETM+ data (30 m resolution)

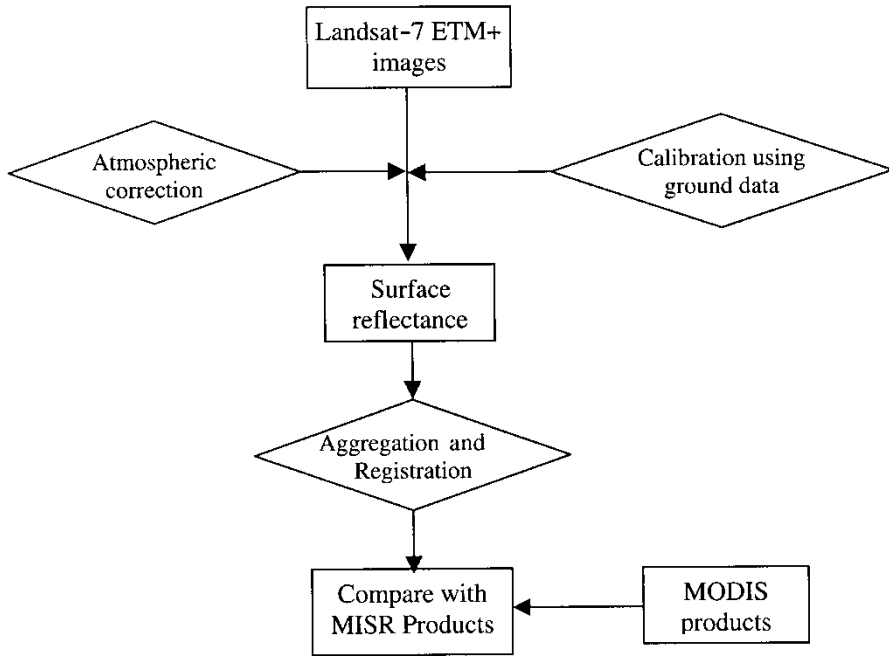


Figure 1. Flowchart of the validation process.

to bridge this gap. The procedure for validating MODIS reflectance and albedo products is to calibrate ETM+ reflectance and albedo products first using ground measurements, and then aggregate and compare them with 1.1 km MISR products (Liang *et al.* 2002a).

2. Field campaign and satellite data

A series of field campaigns were carried out at the USDA Beltsville Agricultural Research Center (BARC), Beltsville, Maryland. BARC is one of the 24 NASA EOS Land Validation Core Sites (Justice *et al.* 1998). The land cover of BARC includes deciduous broadleaf and mixed forest, water, wooded grassland, cropland and some urban. Detailed ground measurements including vegetation structure (LAI, height, stand density, percentage cover), optics (vegetation and soil) and crop yield were made and entered into a Geographical Information System (GIS). Surface reflectance spectral measurements and broadband albedos of a variety of cover types were made with a spectroradiometer (0.4–2.5 μm) and portable albedometers. Surface reflectance and albedos of homogeneous plots of the different cover types were measured within 1 h of the satellite overpass. Landsat-7 and Terra data are acquired over the test site near-simultaneously when the latter had viewing angles very close to nadir. MODIS products of interest for this validation work include directional reflectance from atmospheric correction (MOD09) (Vermeulen and Vermote 1999) and broadband albedos (MOD43B3) (Strahler *et al.* 1999).

Data from 11 May 2000, 5 December 2000 and 22 January 2001 were selected for analysis because of clear-sky conditions and the availability of both MISR and Landsat ETM+ imagery. MOD09, MOD43B3 and MOD43B4 products were

acquired for both 5 December 2000 and 22 January 2001. For 11 May 2000, no MODIS reflectance or albedo products were available. Fluctuations of weather and surface conditions due to differences in times between Landsat-7 and Terra (about 40 min) are assumed to be negligible.

3. Methodology

The comparison of MISR DHR and BHR, BRF and HDRF is straightforward as they have the same resolution, projection and ground coverage. Both ETM+ and MODIS data need to be preprocessed before comparison with MISR products. The ETM+ data were atmospherically corrected to obtain surface reflectance and then registered to MISR resolution. MOD09, MOD43B3 and MOD43B4 were also registered with MISR and integrated to MISR bands. Detailed steps are explained below.

3.1. Atmospheric correction of ETM+ imagery

Because surface reflectance products were already provided by the MODIS science team, atmospheric correction was performed only for Landsat ETM+ data. Spatially varying haze was removed using the method described by Liang *et al.* (2001). This procedure uses a catalogue of atmospheric correction functions stored in look-up tables created with the MODTRAN atmospheric model (Berk *et al.* 1999). The influence of adjacency effect from neighboring pixels was also taken into account. Sunphotometers installed at NASA/Goddard Space Flight Center (GSFC), located within the study area as part of the AERONET (Aerosol Robotic Network) system (Holben *et al.* 1998), provided continuous measurements of aerosol optical depth and column water vapour content of the atmosphere.

The output of the ETM+ atmospheric correction procedure is an at-surface reflectance image for each spectral band. The images were calibrated with simultaneous ground measurements of reflectance that are integrated to provide bandwidths corresponding to the ETM+ spectral bands. Prior validation results (Liang *et al.* 2002b) indicate that the surface reflectance data derived from ETM+ data are accurate.

3.2. Registration and aggregation

A two-step procedure of registration and aggregation was employed to aggregate ETM+/MODIS surface reflectance/albedo to the MISR resolution. Both MODIS and ETM+ images need to be geometrically registered with MISR images. The registration of ETM+ and MISR reflectance data involves the upscaling from ETM+ resolution to MISR resolutions. From numerical experiments using a three-dimensional (3D) atmospheric radiative transfer (RT) model, Liang (2000) found that upscaling of reflectance and albedo products from 30 m to 1 km over vegetated surface is quite linear. It implies that we can linearly average the high-resolution (ETM+) reflectance and albedo products up to the coarse resolutions (MODIS or MISR). The average of 17 by 17 blocks of ETM+ pixels was first calculated to generate an intermediate product at 510 m resolution. The aggregated ETM+ imagery was then registered with the 1.1 km MISR imagery by manually selecting common ground control points.

3.3. Narrowband to broadband albedo conversion

Satellite data are an important tool for obtaining albedo; however, the data are limited by the narrow spectral range of the radiometer and the limited viewing angle. While the MODIS science team provides surface broadband albedo as a standard product, the MISR science team does not. Studies have outlined techniques to estimate surface broadband albedo using more than one satellite channel (Brest and Goward 1987, Saunders 1990, Liang 2001). For example, Liang (2001) developed a validated method for retrieving the broadband surface albedo from narrowband sensors based on radiative transfer simulations. The linear formulae to compute MISR broadband albedos from its spectral albedo used here are:

$$\begin{aligned} a_{\text{vis}} &= 0.381a_1 + 0.334a_2 + 0.287a_3 \\ a_{\text{nir}} &= -0.387a_1 - 0.196a_2 + 0.504a_3 + 0.830a_4 + 0.011 \\ a_{\text{sw}} &= 0.126a_2 + 0.343a_3 + 0.415a_4 + 0.0037 \end{aligned} \quad (1)$$

where a_{vis} , a_{nir} and a_{sw} are the total visible, near-IR and shortwave albedo, respectively, and a_i are the MISR spectral albedos (i.e. the MISR BHR or DHR). As noted in Liang (2001), the fitting formulae for visible and total shortwave albedos are reasonable. The formula for the near-infrared (NIR) is acceptable although MISR has only one band in the NIR spectrum. The formulae for converting ETM+ spectral albedos into broadband albedos are described by Liang (2001). The ETM+ spectral reflectance is equal to the surface spectral albedo assuming the surface is Lambertian. For MODIS, MOD43B3 products are the broadband albedos which are derived from a semi-empirical BRDF model using 16-day observations.

3.4. Data comparison

Since ETM+, MODIS and MISR bands do not have the same spectral response functions, ETM+ and MODIS spectral reflectance were adjusted empirically to MISR reflectance based on their sensor spectral response functions and a surface reflectance spectra library. The statistical relations for this have been established based on analysis of hundreds of surface reflectance spectra of different cover types (Liang 2001). These reflectance spectra were integrated with ETM+, MODIS and MISR sensor spectral response functions and a simple linear regression was then performed. The fitting of the MISR spectral bands using the ETM+ and MODIS bands is presented as figure 2. Two measures were used to characterize the fitting, R-square (R^2) and the rms of error (RSE). The empirical formulae to predict MISR spectral reflectance R_i from ETM+ and MODIS spectral band reflectance (r_i) are as follow.

For ETM+ channels to MISR channels:

$$\begin{aligned} R_1 &= 1.1894r_1 - 0.2521r_2 + 0.0345r_3 + 0.0326r_4 - 0.0380r_5 \\ R_2 &= -0.0244r_1 + 1.1579r_2 - 0.1447r_3 + 0.0085r_4 + 0.0099r_5 \\ R_3 &= 0.1531r_1 - 0.2092r_2 + 1.0522r_3 + 0.0132r_5 + 0.0112r_6 \\ R_4 &= 0.2355r_1 - 0.3017r_2 + 0.0395r_3 + 1.0001r_4 + 0.0574r_5 \end{aligned} \quad (2)$$

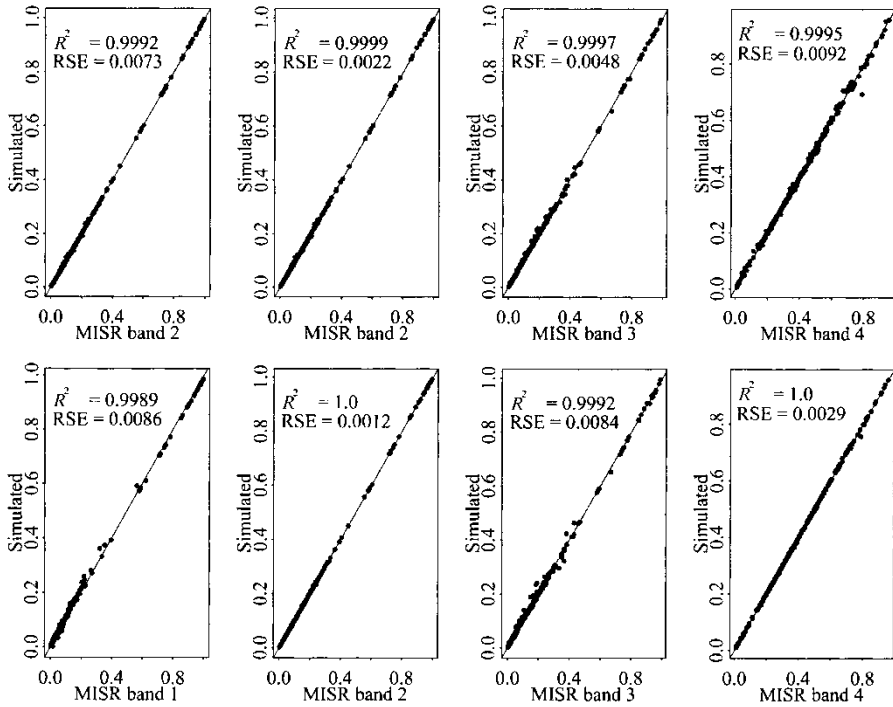


Figure 2. Comparison of MISR bands with simulated ones from ETM+ (top) and MODIS bands (bottom).

For MOD09 channels to MISR channels:

$$\begin{aligned}
 R_1 &= 0.9899r_3 \\
 R_2 &= 0.0723r_1 + 0.0042r_2 - 0.0187r_3 + 0.9431r_4 - 0.0051r_6 \\
 R_3 &= 1.0262r_1 - 0.0152r_2 + 0.1583r_3 - 0.1807r_4 + 0.0530r_6 \\
 R_4 &= 0.9742r_2 + 0.0563r_3 - 0.0490r_4 + 0.0167r_5 + 0.0102r_6
 \end{aligned} \tag{3}$$

4. Results

4.1. Comparison of MISR DHR and BHR data

As the initial part of the validation process, comparisons were made between DHR and BHR. A 250 by 250 pixel mask was used to subset a square homogeneous area of interest from three MISR images. This includes urban, forests, crops and water. Figure 3 shows the R^2 and RSE between DHR and BHR for 22 January 2001. Although the BHR–DHR distribution is a little scattered, especially for band 1, their difference is negligible ($R^2 > 99.7\%$). The highest RSE is 0.013 for band 1. For other bands, the RSE is less than 0.1%. The deviation occurs where the aerosol distribution is spatially irregular and is thus attributed to the aerosol model uncertainties of the retrieval algorithm. Although not shown here, BHR and DHR are almost the same for 5 December 2000. Moreover, there is very little difference in the 11 May 2000 scene.

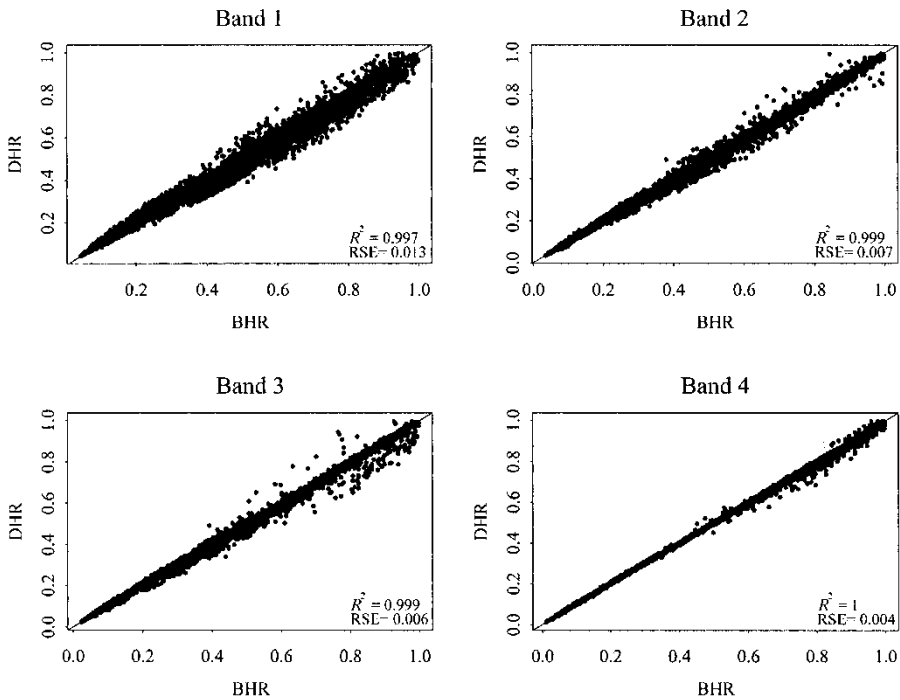


Figure 3. Comparison of MISR DHR and BHR of 22 January 2001.

4.2. Comparison of BRF and HDRF data

A comparison of BRF and HDRF was made for each band at nine different viewing angles. Similar to DHR and BHR, the mean difference between BRF and HDRF is very small (figure 4). For brevity, the 5 December 2000 graph, which displays a perfect match between BRF and HDRF, is not shown here. After checking with the MISR images, deviations from the 1:1 line are found mainly associated with the haze, cloud or shadow regions. For example, in the 22 January 2001 scene, some parts of the image are spoiled by haze and clouds. For hazy regions, the BRF is greater than the HDRF, while the HDRF is greater than the BRF for the cloud shadows and snow areas. For the clear regions, the HDRF and the BRF are nearly the same. For the whole image, there is no general trend whether BRF is greater than HDRF or vice versa.

4.3. Comparing MISR BRF with ETM+ and MODIS data

The Landsat-7 and MODIS data in this experiment were acquired at similar viewing geometry and overpass time. The MISR nadir-view BRF is somewhat comparable with ETM+ and MODIS data. The correlation varies between the ETM+ surface reflectance and MISR nadir-view BRF (figure 5). For example, the R^2 between ETM+ reflectance and MISR BRF is 0.537, 0.89 and 0.759 for band 4 for 11 May 2000, 5 December 2000 and 22 January 2001, respectively (the graph of 11 May 2000 is not shown here). Compared with ETM+, the relationship between MODIS and MISR reflectance is more complicated. There is a strong relationship between MOD09 and MISR nadir-view BRF on 5 December 2000 ($R^2=0.347$,

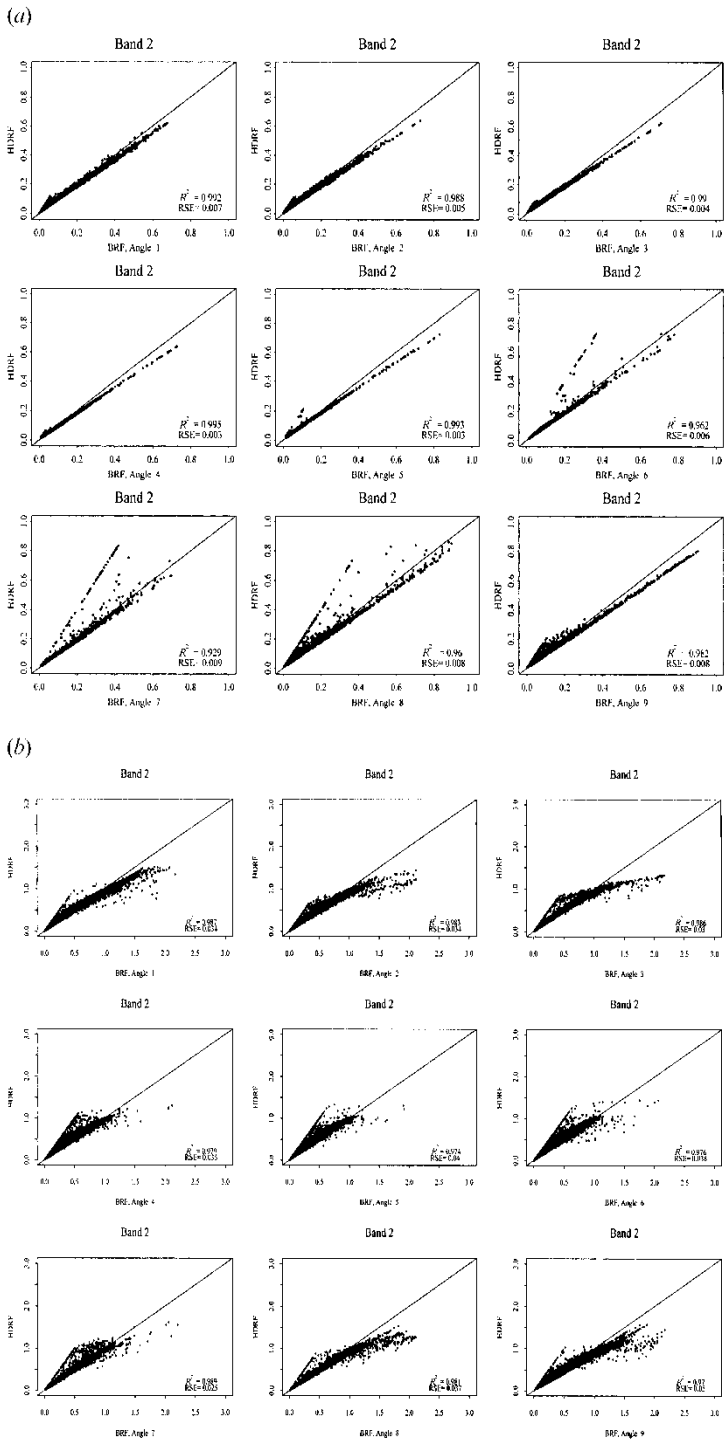


Figure 4. Comparison of MISR BRF and HDRF, band 2 (green) of (a) 5 December 2000 and (b) 22 January 2001. Angles 1–9 represent nine viewing angles (Df, Cf, Bf, Af, An, Aa, Ba, Ca, and Da).

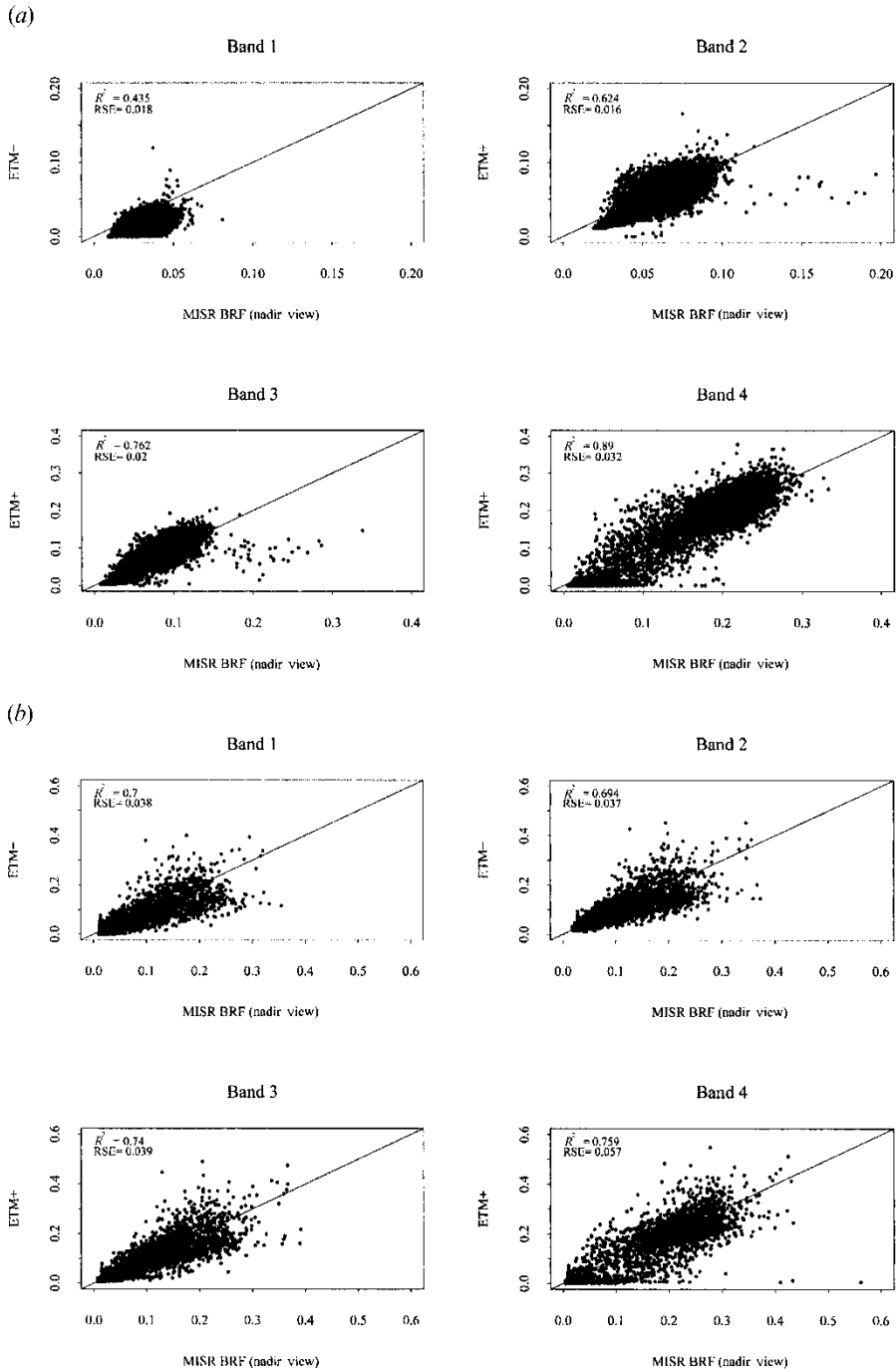


Figure 5. Comparison of MISR BRF (nadir view) and ETM+ retrieved reflectance of (a) 5 December 2000 and (b) 22 January 2001.

0.452, 0.655, 0.842; RSE=0.013, 0.019, 0.023, 0.035), but it is not strong on 22 January 2001 except for band 4 ($R^2=0.277, 0.394, 0.58, 0.288$; RSE=0.072, 0.067, 0.064, 0.14) (figure 6). This may be caused by registration errors, cloudy pixels or snow pixels. The 5 December 2000 image is affected by some clouds, haze and shadows. A large portion of the 22 January 2001 image is covered by cloud and shadow also. Looking into the spatial trend of BRF and MOD09, the nadir-view BRF is greater than MOD09 in the haze and snow regions, yet smaller for shadows. They are very similar for clear areas. Because of the similarity of BRF and HDRF, only BRF is compared above.

4.4. Evaluating surface broadband albedos

There are very strong correlations among broadband albedos from ETM+, MODIS and MISR (figure 7). Note that this figure is for cloud- and haze-free areas only. For both 5 December 2000 and 22 January 2001, the MISR broadband albedo is greater than the broadband albedo derived from ETM+ and MODIS. On 5 December 2000, the MISR albedo is closer to the ETM+ albedo ($R^2=0.836, 0.92, 0.914$; RSE=0.054, 0.04, 0.046) than to the MODIS albedo ($R^2=0.666, 0.597, 0.538$; RSE=0.037, 0.027, 0.027). A very abnormal distribution is seen on 22 January 2001 when the MODIS visible and shortwave albedos are much smaller than MISR ones (ETM+: $R^2=0.173, 0.142, 0.167$; RSE=0.106, 0.067, 0.085. MODIS: $R^2=0.254, 0.364, 0.326$; RSE=0.194, 0.06, 0.124). The deviation could be attributed to the difference between MODIS and MISR 'albedos' as well as the presence of cloud and snow. MISR albedo is integrated from surface reflectance information available from all angular views. The MODIS albedo product treats a pixel as a snow-covered pixel only when the majority of a 16-day period are covered by snow (Strahler *et al.* 1999). Snow pixels present in MISR BHR and ETM+ on 22 January 2001 were not treated as snow in the 16-day MOD43B3 product. The MODIS data quality mask also demonstrates that areas with great albedo uncertainties are indeed the snowy regions on both ETM+ and MISR. It is more apparent in visible and total shortwave band than in NIR band. On 11 May 2001, when it is clear and snow-free for both MISR and ETM+, their correlation is high ($R^2=0.744, 0.687, 0.68$; RSE=0.01, 0.021, 0.012).

5. Conclusions

Under clear-sky conditions, the reflectance difference between BRF and HDRF and the spectral albedo difference between BHR and DHR are not statistically significant. Our preliminary comparison results show that MISR surface reflectance and albedo products are similar to those obtained from ETM+ and MODIS. There are strong relationships between ETM+ surface reflectance and MISR nadir-view BRDF; however, this relationship is affected by the existence of cloud, snow and shadow. For the clear areas, MISR BRF is similar to MOD09 derived reflectance, but is greater for the haze and snow regions and smaller for shadows. The MISR albedo product is closely related to the ETM+ ($R^2 > 83.6\%$, RSE < 0.054) and, to a lesser extent, MODIS ($R^2 > 53.8\%$, RSE < 0.037). MODIS albedo is less than MISR albedos (e.g. on 5 December 2000) due to different snow treatment.

Note that these validation results are based on three clear days and the near nadir-viewing geometry. More work is needed to examine the MISR products for a wide range of surface and atmospheric conditions. AirMISR data, which have great

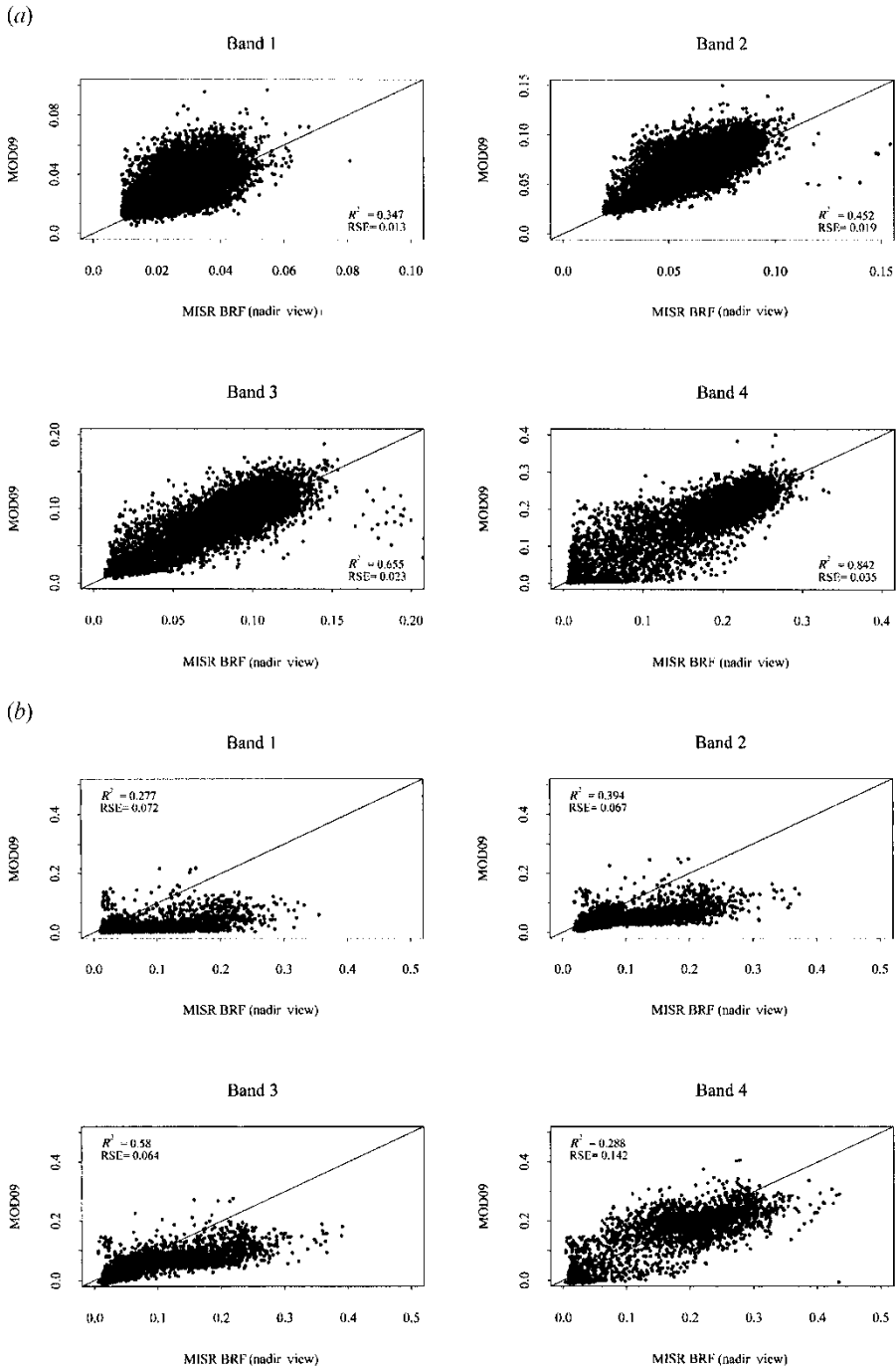


Figure 6. Comparison of MISR BRF (nadir view) and MOD09 data of (a) 5 December 2000 and (b) 22 January 2001.

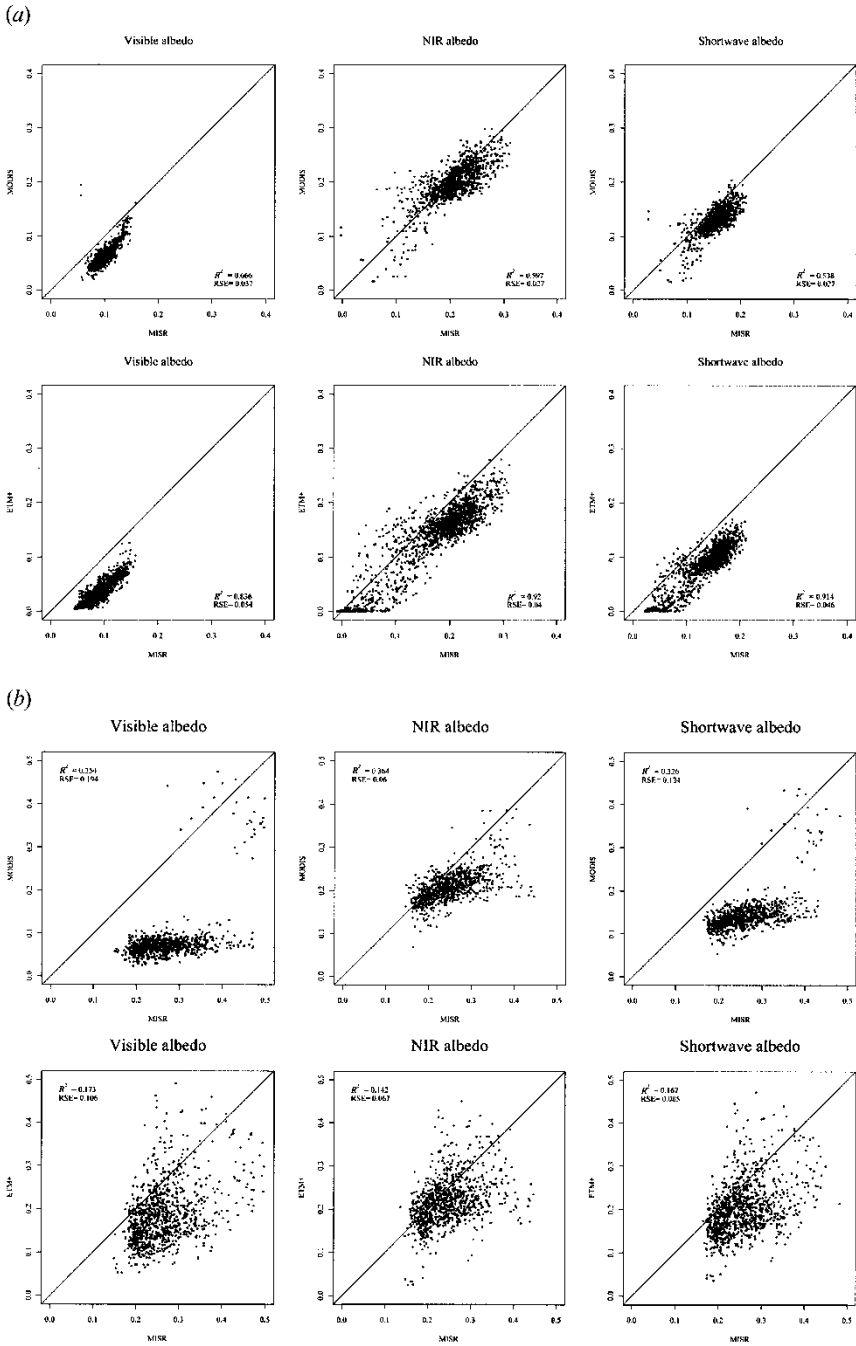


Figure 7. Evaluating MISR albedo with that derived from MODIS and ETM+ of (a) 5 December 2000 and (b) 22 January 2001.

advantage over ETM+ for characterizing the surface directional reflectance at high resolution, have been acquired for the BARC study area and will be used for further validation work. Since the MISR products used in this study are not the final delivery products, the final conclusion about the uncertainties of these products will be made after the MISR data reprocessing.

Acknowledgments

The work is partially funded by NASA EOS validation program under grant NAG5-6459. Chad Shuey, Andy Russ and Wayne Dulaney contributed substantially to the field campaigns. The authors thank the MISR science team at NASA Langley Distributed Active Archive for their efforts to make surface products available to us. The authors also thank the AERONET investigator team for Sunphotometer data.

References

- BERK, A., ANDERSON, G. P., ACHARYA, P. K., CHETWYND, J. H., BERNSTEIN, L. S., SHETTLE, E. P., MATTHEW, M. W., and ADLER-GOLDEN, S. M., 1999, MODTRAN4 users manual. Air Force Research Laboratory, Hanscom AFB, MA.
- BREST, C. L., and GOWARD, S. N., 1987, Deriving surface albedo measurements from narrow band satellite data. *International Journal of Remote Sensing*, **8**, 351–367.
- DINER, D. J., MARTONCHIK, J. V., BOREL, C., GERSTL, S. A. W., GORDON, H. R., KNYAZIKHIN, Y., MYNENI, R., PINTY, B., and VERSTRAETE, M. M., 1999, Multi-angle Imaging Spectro-Radiometer (MISR) level 2 surface retrieval (MISR-10) algorithm theoretical basis, Jet Propulsion Laboratory, California Institute of Technology.
- GU, X. F., and GUYOT, G., 1993, Effect of diffuse irradiance on the reflectance factor or reference panels under field conditions. *Remote Sensing of Environment*, **45**, 249–260.
- HOLBEN, B. N., ECK, T., SLUTSKER, I., TANRE, T., BUIS, J., SETZER, A., VERMOTE, E., REAGAN, J., KAUFMAN, Y., NAKAJIMA, T., LAVENU, F., JANKOWIAK, I., and SMIRNOV, A., 1998, AERONET—a federated instrument network and data archive for aerosol characterization. *Remote Sensing of Environment*, **66**, 1–16.
- JUSTICE, C., STARR, D., WICKLAND, D., PRIVETTE, J., and SUTTLES, T., 1998, EOS land validation coordination: an update. *Earth Observer*, **10**, 55–60.
- LIANG, S., 2000, Numerical experiments on spatial scaling of land surface albedo and leaf area index. *Remote Sensing Reviews*, **19**, 225–242.
- LIANG, S., 2001, Narrowband to broadband conversions of land surface albedo I—Algorithms. *Remote Sensing of Environment*, **76**, 213–238.
- LIANG, S., FANG, H., and CHEN, M., 2001, Atmospheric correction of Landsat ETM+ land surface imagery: I. methods. *IEEE Transactions on Geoscience and Remote Sensing*, **39**, 2490–2498.
- LIANG, S., FANG, H., CHEN, M., WALTHALL, C., DAUGHTRY, C., MORISSETTE, J., SCHAAF, C., and STRAHLER, A., 2002a, Validating MODIS land surface reflectance and albedo products: methods and preliminary results. *Remote Sensing of Environment*, **83**, 149–162.
- LIANG, S., FANG, H., MORISSETTE, J., CHEN, M., WALTHALL, C., DAUGHTRY, C., and SHUEY, C., 2002b, Atmospheric correction of Landsat ETM+ land surface imagery: II. validation and applications. *IEEE Transactions on Geoscience and Remote Sensing*, **40**, 2736–2746.
- LUCHT, W., 1998, Expected retrieval accuracies of bidirectional reflectance and albedo from EOS-MODIS and MISR angular sampling. *Journal of Geophysical Research*, **103**, 8763–8778.
- SAUNDERS, R. W., 1990, The determination of broad band surface albedo from AVHRR visible and near-infrared radiances. *International Journal of Remote Sensing*, **11**, 49–67.
- STRAHLER, A. H., LUCHT, W., SCHAAF, C. B., TSANG, T., GAO, F., LI, X., MULLER, J. P.,

- LEWIS, P., and BARNLEY, M. J., 1999, MODIS BRDF/albedo product: algorithm theoretical basis document version 5.0, National Aeronautics and Space Administration.
- VERMOTE, E. F., and VERMEULEN, A., 1999, Atmospheric correction algorithm: spectral reflectances (MOD09), National Aeronautics and Space Administration.